High D/H ratios in water and alkanes in comet 67P/Churyumov-Gerasimenko measured with Rosetta/ROSINA DFMS

D. R. Müller[1], K. Altwegg[1], J. J. Berthelier[2], M. Combi[3], J. De Keyser[4], S. A. Fuselier[5,6], N. Hänni[1], B. Pestoni[1], M. Rubin[1], I. R. H. G. Schroeder I[1], and S. F. Wampfler[7]

[1] Physikalisches Institut, University of Bern, Sidlerstrasse 5, 3012 Bern, Switzerland
e-mail: daniel.mueller@unibe.ch
[2] Laboratoire Atmosphères, Milieux, Observations Spatiales (LATMOS), 4 Avenue de Neptune, 94100 Saint-Maur, France
[3] Department of Climate and Space Sciences and Engineering, University of Michigan, 2455 Hayward, Ann Arbor, MI 48109, USA
[4] Royal Belgian Institute for Space Aeronomy, BIRA-IASB, Ringlaan 3, 1180 Brussels, Belgium
[5] Space Science Directorate, Southwest Research Institute, 6220 Culebra Rd., San Antonio, TX 78228, USA
[6] Department of Physics and Astronomy, The University of Texas at San Antonio, San Antonio, TX 78249, USA
[7] Center for Space and Habitability, University of Bern, Gesellschaftsstrasse 6, 3012 Bern, Switzerland

ABSTRACT

Context. Isotopic abundances in comets are key to understanding and reconstructing the history and origin of material in the Solar System. Data for deuterium-to-hydrogen (D/H) ratios in water are available for several comets. However, no long-term studies of the D/H ratio in water of a comet during its passage around the Sun have been reported thus far. Linear alkanes are important organic molecules that have been found on several Solar System bodies, including comets. To date, the processes of their deuteration are still poorly understood, only the upper limits of isotopic ratios for D/H and $^{13}C/^{12}C$ in linear alkanes are currently available.
Aims. The aim of this work is to carry out a detailed analysis of the D/H ratio in water as a function of cometary activity and spacecraft location above the nucleus. In addition, a first determination of the D/H and $^{13}C/^{12}C$ ratios in the first four linear alkanes, namely, methane (CH_4), ethane (C_2H_6), propane (C_3H_8), and butane (C_4H_{10}) in the coma of 67P/Churyumov-Gerasimenko is provided.
Methods. We analysed in situ measurements from the Rosetta/ROSINA Double Focusing Mass Spectrometer (DFMS).
Results. The D/H ratio from HDO/H_2O and the $^{16}O/^{17}O$ ratio from $H_2^{16}O/H_2^{17}O$ did not change during 67P's passage around the Sun between 2014 and 2016. All D/H ratio measurements were compatible within 1σ, with the mean value of 5.01×10^{-4} and its relative variation of 2.0%. This suggests that the D/H ratio in 67P's coma is independent of heliocentric distance, level of cometary activity, or spacecraft location with respect to the nucleus. Additionally, the $^{16}O/^{17}O$ ratio could be determined with a higher accuracy than previously possible, yielding a value of 2347 with a relative variation of 2.3%. For the alkanes, the D/H ratio is between 4.1 and 4.8 times higher than in H_2O, while the $^{13}C/^{12}C$ ratio is compatible, within the uncertainties, with the available data for other Solar System objects. The relatively high D/H ratio in alkanes is in line with results for other cometary organic molecules and it suggests that these organics may be inherited from the presolar molecular cloud from which the Solar System formed.

Key words. Comets: general — Comets: individual: 67P/Churyumov-Gerasimenko – Instrumentation: detectors – Methods: data analysis – Astrochemistry

1. Introduction

Comets are considered as reservoirs of material preserved from the early Solar System. By making this material available to in situ exploration, cometary science contributes important information on the history of the Solar System (Drozdovskaya et al. 2019; Mumma & Charnley 2011). Investigating the isotopic abundances of different elements in various molecules in comets is essential, as the isotopic ratios are sensitive to the environmental conditions at the time of the molecules' formation and they provide crucial information for improving our understanding of the origins of cometary material (Biver et al. 2019; Bockelée-Morvan et al. 2015; Hässig et al. 2017).

The best-studied comet to date is comet 67P/Churyumov-Gerasimenko (hereafter, 67P), a Jupiter-family comet (JFC) that was followed by the Rosetta spacecraft during its orbit around

the Sun. In August 2014, Rosetta rendezvoused with 67P at a heliocentric distance of around 3.6 au. It then accompanied the comet through its perihelion at 1.24 au from the Sun and followed the orbit of 67P back out to a distance of almost 4 au, whereupon the spacecraft intentionally soft-landed on the comet's surface at the end of September 2016. The Rosetta spacecraft, as part of a mission launched and operated by the European Space Agency (ESA), helped uncover a great store of new knowledge about 67P, such as its gas and dust composition (e.g. Herny et al. 2021; Longobardo et al. 2020; Pestoni et al. 2021), nucleus surface (e.g. Feller et al. 2019) and temporal evolution (e.g. Combi et al. 2020; Läuter et al. 2020; Rubin et al. 2019). With its lander, Philae, it was even able to acquire gas and volatiles in dust composition data directly on or near the comet's surface by the COSAC (Goesmann et al. 2015) and Ptolemy (Wright et al. 2015) instruments. No prior cometary ob-

servation has ever been performed for as long a duration and with as high a measurement sensitivity as the Rosetta mission.

The Rosetta spacecraft carried several instrument packages on board, one of which was the Rosetta Orbiter Spectrometer for Ion and Neutral Analysis (ROSINA). ROSINA was comprised of two mass spectrometers, the Double Focusing Mass Spectrometer (DFMS) and a Reflectron-type Time-Of-Flight mass spectrometer (RTOF), in addition to the COmet Pressure Sensor (COPS). In particular, DFMS was used for measurements of the molecular and isotopic composition of cometary volatiles (Balsiger et al. 2007). Hässig et al. (2017) showed that the instrument had a sensitivity, dynamic range and mass resolution high enough to detect even trace amounts of rare isotopologues alongside their more abundant counterparts. It has been used by many authors to investigate the isotopic ratios of sulfur (Calmonte et al. 2017; Hässig et al. 2017), carbon (Hässig et al. 2017; Altwegg et al. 2020), the halogens bromine and chlorine (Dhooghe et al. 2017), and oxygen (Altwegg et al. 2020; Hässig et al. 2017; Schroeder et al. 2019b) in 67P. Altwegg et al. (2015, 2017) used it to measure the D/H ratio in water in 67P's coma, using data from the beginning and near the end of the Rosetta mission. Both measurements were consistent within the uncertainties. From HDO/H$_2$O, a D/H ratio of $(5.3 \pm 0.7) \times 10^{-4}$ was deduced. This is more than three times the terrestrial Vienna Standard Mean Ocean Water (VSMOW) value of 1.5576×10^{-4}, and one of the highest ever measured in a JFC.

Both measurements by Altwegg et al. (2015, 2017) were performed at times when 67P was relatively far from the Sun. The first had relied on data from well before perihelion, in August-September 2014 at a heliocentric distance of 3.4 au, while the second evaluated data from December 2015 at 2 au and the outbound equinox in March 2016 at 2.6 au. Due to the large heliocentric distances of 67P during these measurements, the question arises as to whether the HDO/H$_2$O ratio would differ at smaller heliocentric distances, when a large increase in sublimation from the surface of the cometary nucleus occurred and fresh layers of the comet's surface were likely exposed. Additionally, different cometary hemispheres were active at different times. At greater heliocentric distances, most of the water outgassed came from the comet's northern latitudes. Conversely, closer to perihelion, the contributions of the southern latitudes were more significant (Keller et al. 2015). Schroeder et al. (2019a) investigated the difference between the comet's two lobes and concluded that no significant difference in the D/H ratio could be observed.

A comparison of different Solar System objects shows a broad variation in D/H ratios, with most objects being enriched in deuterium compared to the protosolar nebula (Altwegg et al. 2015). Different potential mechanisms have been proposed to explain these large variations, for instance solar wind induced water formation and isotopic fractionation. Daly et. al (2021) has stated that isotopically light water reservoirs could have been produced by solar wind implantation into fine-grained silicates. The authors concluded that this may have been a particularly important process in the early Solar System, thus potentially providing a means to recreate Earth's current water isotope ratios. On the other hand, the isotopic fractionation describes the variation in abundances of the isotopes of an element. It arises from both physical and chemical processes and is also temperature-dependent for some molecules. According to Kavelaars et al. (2011), the main reservoir of deuterium in the protosolar nebula was molecular hydrogen with a D/H ratio of 1.5×10^{-5}. Ion-molecule reactions in the interstellar medium or grain surface chemistry can cause fractionation among deuterated species. In the pre-solar cloud, fractionation resulted in molecules being en-
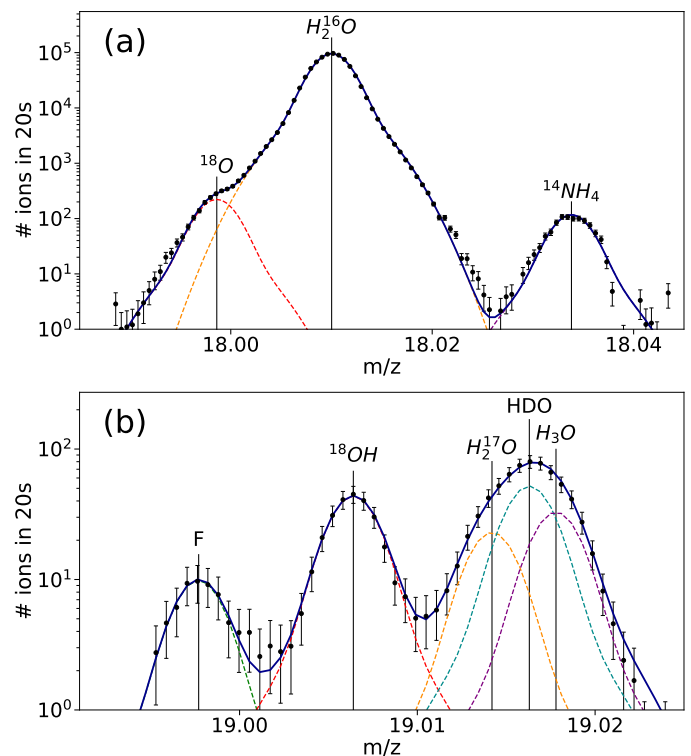

Fig. 1. Sample mass spectra for *m/z* 18 and 19 displaying the signatures of the isotopologues of water. *Panel a*: *m/z* 18 from 2015-05-07 17:38 (UTC). *Panel b*: *m/z* 19 from 2015-05-26 01:35 (UTC). Measured data are represented by black dots including their statistical uncertainties. Individual mass fits and the total sum of the fits are shown with coloured lines.

riched in deuterium. Isotopic exchange reactions with H$_2$ in the gas phase of the solar nebula would then lower this enrichment. Various authors suggested that the enrichment in deuterium increases with increasing heliocentric distance (Furuya et al. 2013; Kavelaars et al. 2011; Geiss & Reeves 1981). Comets are assumed to be a source of primordial material from the early Solar System (Wyckoff 1991). Consequently, knowledge of variations in the deuterium enrichment in comets is of high importance, as their compositions are indicative of their regions of origin and the environmental conditions during their formation (Hässig et al. 2017).

Ground-based observations of deuterated water in comet C/2014 Q2 (Lovejoy), appeared to show a change in the D/H ratio in water from pre- to post-perihelion (Paganini et al. 2017). Paganini et al. (2017) measured a post-perihelion D/H ratio of $(3.02 \pm 0.87) \times 10^{-4}$, which was significantly higher than the pre-perihelion value of $(1.4 \pm 0.4) \times 10^{-4}$ measured by Biver et al. (2016). Two explanations for this discrepancy were put forward by Paganini et al. (2017): (1) the ratio of D/H in water changed after perihelion or (2) the D/H ratio in water might have been strongly influenced by a systematic bias in the estimate as different experimental setups were applied. Paganini et al. (2017) used the Near Infrared Spectrograph (NIRSPEC) at the 10-meter W. M. Keck Observatory (Keck II) for their infrared measurements. In contrast, Biver et al. (2016) used radio/sub-mm observations from the IRAM 30 m radio telescope and the Odin 1.1 m sub-millimeter satellite. The two different approaches and the use of two telescopes with different beam sizes in the measurements by Biver et al. (2016) could provide a possible explanation for the varying D/H results in this comet.

A recent study of the D/H ratio in comets showed that the D/H ratio correlates with the nucleus' active area fraction (Lis et al. 2019). According to the authors' definition, comets with an active fraction larger than 0.5 are called hyperactive comets and typically exhibit D/H ratios in water consistent with the terrestrial value. The authors argue that these hyperactive comets require an additional source of water vapour within their comae, which might be explained by the presence of subliming icy grains ejected from the nucleus. There exist other definitions of hyperactivity in comets, such as in Sunshine & Feaga (2021), and thus the classification of 67P as hyperactive or not is not always clear. Fulle (2021) has hypothesised that the correlation of the D/H ratio with the nucleus' active area fraction might be due to a mixture of water-rich and water-poor pebbles. The author states that the two kinds of pebbles contain different D/H ratio values due to their initial formation conditions. He also suggests that the D/H average in the nuclei may differ from the values measured in cometary comae and can therefore not be obtained by local sample-return missions. According to the author, cryogenic return missions would sample water-rich and water-poor pebbles separately, which would only be representative of their corresponding water-rich or water-poor regions, respectively. A cometary average therefore cannot be measured by local sampling.

This work is the first to assess the scenario of a changing D/H ratio in a comet with numerous data points from in situ measurements spread over a long time period and shall answer the question of whether the D/H ratio in comets is dependent on heliocentric distance, phase angle or gas production rate. To do so, we evaluated the full mission data of ROSINA/DFMS to investigate the D/H ratio in HDO and H_2O over one third of 67P's orbit. The evaluated mission phases are specified in Table 1.

In addition to water, the D/H ratios of different alkanes have been studied. Alkanes are acyclic saturated hydrocarbon molecules containing only single carbon-carbon bonds. They have been found on several Solar System bodies, including the Earth, and in the atmospheres of the giant planets and Saturn's moon Titan (Clark et al. 2009; Lunine & Atreya 2008). The isotopic ratios in these organic compounds are of special interest as they may provide not only an insight into the chemical and physical conditions before and during the formation of the Solar System, but can also constrain the delivery of organic matter by comets to the early Earth (Doney et al. 2020; Rubin et al. 2019; Schuhmann et al. 2019).

2. Instrumentation and methodology

The ROSINA/DFMS is a Nier-Johnson type double focusing mass spectrometer with a high mass resolution of m/Δm = 3000 at the 1%-level on the mass-to-charge ratio (m/z) 28 (Balsiger et al. 2007). In the DFMS, incoming neutral gas is ionised by electron impact with an electron energy of 45 eV. Most ions formed are singly charged. For this reason, the charge state will not be indicated in the following, except for the subset of doubly charged ions, such as H_2S^{++}. The newly formed ions are accelerated through a 14 μm slit, deflected by 90 degrees in a toroidal electrostatic analyser and, finally, they undergo a 60 degree deflection in the field of a permanent magnet. With the combination of the different fields, the instrument is tuned to the level that only ions with a specific mass-to-charge ratio make it through the analyser section. The remaining ion beam is amplified by two micro channel plates (MCP) in a Chevron configuration. The electron packet issued from the MCP is finally collected by a position-sensitive Linear Electron Detector Array (LEDA). The
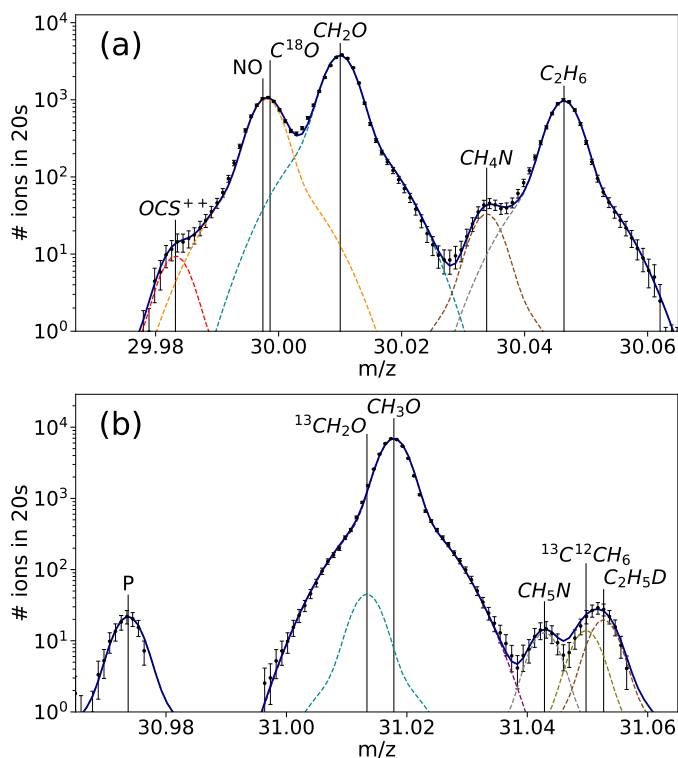

Fig. 2. Sample mass spectra for *m/z* 30 and 31 showing the signatures of the isotopologues of ethane. *Panel a*: *m/z* 30 from 2014-03-10 19:36 (UTC). The peaks of NO and $C^{18}O$ could not be resolved and appear as one peak (orange line). *Panel b*: *m/z* 31 from 2014-03-10 19:37 (UTC). Measured data are represented by black dots including their statistical uncertainties. The individual mass fits and the total sum of the fits are shown with coloured lines.

LEDA consists of two rows of 512 pixels each (Nevejans et al. 2002).

The MCP potential difference can be varied to adjust its amplification. The amplification is the gain of the MCP. 16 different settings or gain steps can be chosen from default voltages. Due to detector ageing, the gains associated with each voltage settings are not constant over time. This has to be accounted for when comparing DFMS data with different gain steps. In addition, the unequal usage of the 512 pixels of the LEDA causes a position-dependent degradation of the detector over time. For this reason, a pixel gain correction needs to be implemented during data evaluation (De Keyser et al. 2019). Gain and pixel gain correction factors are evaluated in Schroeder et al. (2019b).

A single spectrum comprises a range of *m/z* around a specified integer *m/z*. For *m/z* 28, this is ±0.25. DFMS spectra are fitted on individual mass lines using the sum of two Gaussian peaks (double Gaussian distribution). The second Gaussian depends on the first one as its signal amplitude is approximately 10% of the first Gaussian and its width is about three times broader than the narrow first Gaussian. All peaks on the same spectrum are characterised by the same width and height ratios of the two Gaussian distributions. The interdependence of the two Gaussians is known from thorough calibration measurements by Le Roy et al. (2015) and Hässig et al. (2013, 2015), wherein the combined influence of the molecular ionisation cross-sections, the mass-dependent instrument transfer function, isotope-dependent fractionation patterns due to the electron impact ionisation, and detector yields have been investigated. Their effects are included in the systematic error calculations.

Table 1. D/H in H_2O during different mission phases and compared to previous evaluations.

Mission Phase	Dates	D/H in H_2O	Heliocentric distance [au]	# of evaluated spectra
First equinox	May 2015	$(5.03 \pm 0.17) \cdot 10^{-4}$	1.71 - 1.52	44
Perihelion	August 2015	$(5.01 \pm 0.20) \cdot 10^{-4}$	1.24	37
Peak gas production	2015-08-30	$(4.98 \pm 0.25) \cdot 10^{-4}$	1.26	22
Second equinox	March 2016	$(5.02 \pm 0.17) \cdot 10^{-4}$	2.45 - 2.65	47
Relative mean ratio		$(5.01 \pm 0.10) \cdot 10^{-4}$		150
Absolute mean ratio		$(5.01 \pm 0.41) \cdot 10^{-4}$		150
Pre-first equinox [a]	Aug. / Sep. 2014	$(5.3 \pm 0.7) \cdot 10^{-4}$	≈ 3.4	26
Pre-second equinox [b]	Dec. 2015 / Mar 2016	$(5.25 \pm 0.7) \cdot 10^{-4}$	2.0 & 2.6	18

References. (a) Altwegg et al. (2015); (b) Altwegg et al. (2017).

Finally, a mass scale may be applied to the spectrum such that each pixel corresponds to a certain mass. The mass scale is applied as described in detail in Calmonte et al. (2016).

Formally, for each pixel p_i corresponding to a LEDA pixel in the DFMS mass spectrum, the counted number of particles, counts(pi), can be described as:

$$\text{counts}(p_i) = a_1 e^{-(\frac{p_i - p_0}{c_1})^2} + a_2 e^{-(\frac{p_i - p_0}{c_2})^2}, \tag{1}$$

with a_1 and a_2 being the amplitudes of the first and the second Gaussian, respectively, p_0 the pixel zero corresponding to the integer mass (center pixel), and c_1 and c_2 the widths of the two Gaussians. The total number of particles impinging on the detector is represented by the peak area. It is given by the integral of the fitted double-Gaussian distribution:

$$\text{\# of particles} = \int_{-\infty}^{+\infty} \text{counts}(p) \, dp = \sqrt{\pi}(a_1 c_1 + a_2 c_2). \tag{2}$$

Figures 1 and 2 show examples of fitted mass spectra after application of the mass scale. The error bars show the statistical uncertainty on the count number.

Data from different periods during the Rosetta mission have been investigated. The HDO/H_2O ratio in 67P has been examined at the first equinox (May 2015), at perihelion (August 2015), at the time of the peak gas production (end of August and early September 2015), and at the second equinox (March 2016) of 67P. These characteristic time periods have been chosen in order to determine a potential heliocentric distance dependence on the HDO/H_2O ratio.

In addition, the D/H ratios of the simplest four linear alkanes - methane (CH_4), ethane (C_2H_6), propane (C_3H_8) and butane (C_4H_{10}) - have been studied at times when the alkane signals were clearly visible in the respective spectra. Butane has two structural isomers, n-butane and iso-butane, which have the same molecular formula, but with the atoms in a different order. They cannot be distinguished from each other with the DFMS and thus no distinction is made in the following. Methane and ethane have previously been detected in several comets (C/1996 B2 (Hyakutake): Mumma et al. 1996; 153P/Ikeya-Zhang: Kawakita et al. 2003; C/2007 N3 (Lulin): Gibb et al. 2012) and upper limits for their D/H ratios have been reported (Bonev et al. 2009; Doney et al. 2020). Propane and butane were first detected in 67P by Schuhmann et al. (2019). These authors have also published the relative abundances of the simplest four linear alkanes compared to methane and water in 67P's coma for two different time periods. The abundances relative to water are shown in Table 2. The

Table 2. Relative abundance of alkanes in 67P. Data from Schuhmann et al. (2019).

Species	Abundance relative to water [H_2O]	
	May 2015	May 2016
Methane	$(3.43 \pm 0.68) \cdot 10^{-3}$	$(6.48 \pm 1.30) \cdot 10^{-2}$
Ethane	$(2.92 \pm 0.58) \cdot 10^{-3}$	$(5.13 \pm 1.03) \cdot 10^{-1}$
Propane	$(1.80 \pm 0.36) \cdot 10^{-4}$	$(2.75 \pm 0.55) \cdot 10^{-2}$
Butane	not detected	$(5.28 \pm 1.06) \cdot 10^{-3}$

abundance of the simplest four linear alkanes strongly increased from pre- to post-perihelion. No D/H ratios for any of the alkanes considered have been reported to date.

Two sources of uncertainty are relevant for DFMS data analysis: statistical uncertainties in the count rates and systematic uncertainties due to instrumental effects. The statistical uncertainties of the detector counts are proportional to $\sqrt{N}$ for N counts. Additionally, a fitting error has been included in the case of overlapping peaks. This fitting error accounts for a possible ambiguity when peaks cannot be clearly separated and depends on the relative peak intensities and the mass difference between the peaks. Instrumental effects, arising from pixel-dependent degradation (pixel gain correction) and changes in the detector gain over time, are systematic uncertainties. The uncertainty of the pixel gain is 5% and the uncertainty of the overall gain is 6%. These values were previously derived and applied by Schroeder et al. (2019b). The statistical and fitting uncertainties are considered for each individual measurement point. Uncertainties in the detector and pixel gain, which are of a systematic nature, are only considered for the absolute mean ratios. In the case of HDO/H_2O, the overall gain has a large impact on the evaluation as *m/z* 18 has always been measured on a smaller gain step than *m/z* 19. For the alkanes, the gain uncertainty has to be included for methane and propane. The isotopologues of ethane and butane on the other hand were measured on the same gain step as their main isotopologues and gain corrections are therefore unnecessary. The pixel gain uncertainty, however, applies to all uncertainty calculations.

3. Results

An extensive analysis of spectra with *m/z* 18 and *m/z* 19 in the coma of 67P showed constant D/H and $^{16}O/^{17}O$ ratios in water
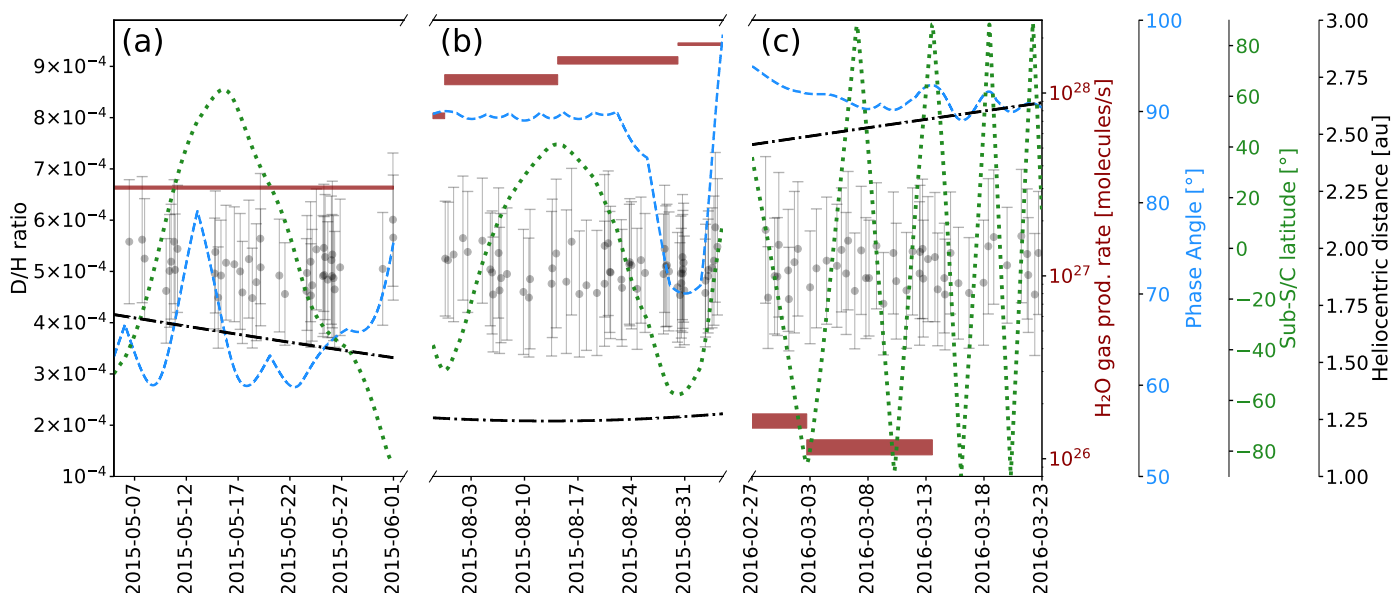
Fig. 3. D/H in H_2O during different mission phases compared to H_2O gas production (Läuter et al. 2020, red), phase angle (blue), sub-S/C latitude (green) and heliocentric distance (black). *Panel a*: First equinox; *Panel b*: Perihelion and peak gas production phase; *Panel c*: Second equinox. The individual measurement uncertainties represent statistical errors from the count rates and errors from the fit.

during the comet's course around the Sun in 2015 and 2016. Furthermore, the D/H and $^{13}C/^{12}C$ ratios in the simplest four linear alkanes could be resolved. This section summarises the results for each of the aforementioned ratios and explains how the results have been obtained.

3.1. HDO/H_2O

A total of 150 spectra around m/z 18 and m/z 19 have been investigated. These spectra contain the signatures of $H_2^{16}O$, $H_2^{17}O$ and HDO. Sample spectra for m/z 18 and m/z 19 are shown in Fig. 1. Using the values from $H_2^{16}O$ and HDO, measured back-to-back within one minute, allows us to derive the D/H ratio from HDO/H_2O as:

$$D/H = \frac{1}{2} \frac{n_{HDO}}{n_{H_2\,^{16}O}}. \quad (3)$$

The goal of this work was to investigate the D/H ratio in water over the whole mission. Therefore, Rosetta data from the first equinox, perihelion, the time of the peak gas production, and the second equinox have been evaluated as specified in Table 1. These data sets span a wide range of heliocentric distances, observational phase angles, water production rates and sub-spacecraft (sub-S/C) latitudes.

The relative mean D/H ratios for the specified mission phases, considering only statistical and fit uncertainties, are shown in Table 1. The mean values are weighted means with the weight for each individual point being inversely proportional to its statistical uncertainty. This improves the results by giving more weight to more precise measurement points. The relative overall mean value was found to be $(5.01 \pm 0.10) \times 10^{-4}$. All periods are consistent with this mean value within the 1σ uncertainty of 2.0%. There is no observable trend between the periods in the D/H value. This suggests that the D/H ratio in 67P's coma remains constant throughout the entire Rosetta mission phase, covering one third of 67P's orbit. Additionally, considering the broad diversity of the conditions under which the data have been observed, the D/H ratio in 67P's coma seems to be independent

of heliocentric distance, level of cometary activity, and observational phase angle, as well as sub-S/C latitudes. The D/H ratio did not even significantly change during extreme situations such as a maximally active southern hemisphere or a phase angle of almost 70. Figure 3 shows the individual D/H ratio data points alongside their corresponding H_2O gas production rate (Läuter et al. 2020), phase angle, latitude and cometary distance to the Sun. For the H_2O gas production, Läuter et al. (2020) reported minimum and maximum values according to their uncertainty estimation. No H_2O gas production values were reported by these authors for the time between 13 March 2016 and the end of the measurements during the second equinox. Combi et al. (2020) provided gas production values for individual measurement points acquired with a different approach, with their results for the overall variation of the H_2O gas production rate being in reasonable agreement with Läuter et al. (2020).

For the absolute value, the systematic uncertainty is added. This systematic uncertainty affects all data points equally and leads to an absolute mean D/H ratio of $(5.01 \pm 0.40) \times 10^{-4}$. This is consistent with the previously published values of $(5.3 \pm 0.7) \times 10^{-4}$ found by Altwegg et al. (2015, 2017). These earlier values were determined before a better understanding of the behaviour of the pixel gain and the overall gain of the DFMS over time was available (De Keyser et al. 2019; Schroeder et al. 2019b). By extending the number of spectra from 26 and 18 in Altwegg et al. (2015) and Altwegg et al. (2017), respectively, to 150 spectra in this work, and thanks to the improved characterisation of the DFMS over time, we were able to improve on the uncertainty. For statistical reasons, this uncertainty is inversely proportional to the square root of the number of spectra and thus greatly decreased by the large number of spectra considered here.

3.2. $^{16}O/^{17}O$

In addition to the signature of HDO, $H_2^{17}O$ has been measured on m/z 19. Together with the already examined $H_2^{16}O$ on m/z 18, the isotopic ratio of $^{16}O/^{17}O$ could be derived. This has already been done by Schroeder et al. (2019b) in a "note added in proof."

Table 3. $^{16}O/^{17}O$ in water during different mission phases.

Mission Phase	$^{16}O/^{17}O$
First equinox	2317 ± 91
Perihelion	2318 ± 115
Peak gas production	2398 ± 141
Second equinox	2379 ± 97
Relative mean ratio	2347 ± 53
Absolute mean ratio	2347 ± 191

However, the authors only investigated data from two distinct dates and only used 35 spectra. With the 150 spectra investigated for the time periods given in Table 1, an updated value can now be presented. Table 3 shows the relative mean $^{16}O/^{17}O$ ratios for the different mission phases, considering only statistical and fit uncertainties. As in Section 3.1, the mean values are weighted means and the uncertainty is inversely proportional to the square root of the number of spectra. The relative overall mean value over all evaluated spectra was found to be 2347 ± 53. All the periods are consistent with this mean value within the 1σ uncertainty of 2.3%. There is no observable trend in the $^{16}O/^{17}O$ ratio among the periods considered. This is in line with the invariability of the $^{16}O/^{18}O$ ratio in Schroeder et al. (2019b). It is, however, in contrast with their average values for the $^{16}O/^{17}O$ ratios, as their $^{16}O/^{17}O$ ratio for the first date is approximately 40% higher than the $^{16}O/^{17}O$ ratio for the second date. An explanation for this might be that Schroeder et al. (2019b) did not include $H_3^{16}O$ in their evaluation of m/z 19 spectra. However, all three molecules, $H_2^{17}O$, HDO and $H_3^{16}O$, need to be included in the analysis as their peaks overlap significantly and the influence of $H_3^{16}O$ should not be ignored. Including the systematic uncertainties of the gains affecting all data points equally, gives an absolute mean $^{16}O/^{17}O$ ratio of 2347 ± 191. This represents an approximately 11% enrichment of ^{17}O compared to the value for terrestrial water of (2632 ± 69) (Meija et al. 2016) and is in line with the enrichment of ^{18}O in 67P's coma (Schroeder et al. 2019b). The $^{16}O/^{17}O$ ratio we derived is compatible within the uncertainties with the value reported in the "note added in proof" in Schroeder et al. (2019b).

3.3. Linear alkanes

The D/H and $^{13}C/^{12}C$ ratios of the first four linear alkanes, namely, methane, ethane, propane and butane, have been evaluated. For all alkanes, CnHy, taking into account the statistical correction for the different possible positions of the rare isotopes in the molecule, the D/H and $^{13}C/^{12}C$ ratios are obtained by dividing the measured abundance ratios by $1/y$ and $1/n$, respectively. The alkanes were not always at a detectable level over the entire mission. This required an individual selection of suitable time periods for each of the molecules. For each hydrocarbon, the results will be presented separately in the following subsections.

3.3.1. Methane (CH$_4$)

The methane (CH$_4$) signature was observed clearly from mid-August 2016 until the beginning of September 2016. Hence, 12 spectra from this time period have been evaluated. Spectra with m/z 16 and m/z 17 have been investigated. Sample spectra are shown in Fig. A.1. The m/z 16 spectra used gain step 15, whereas
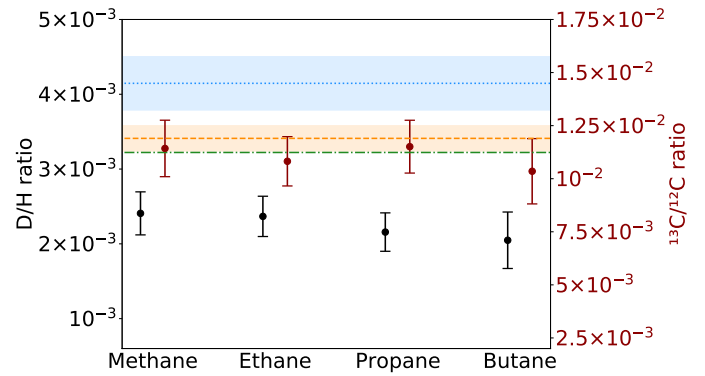
Fig. 4. D/H (black) and $^{13}C/^{12}C$ (red) ratios of the first four linear alkanes compared with $^{13}C/^{12}C$ values in 67P's CO_2 (Hässig et al. 2017, orange), in the Earth (Wilson 1999, green) and in the local ISM (Wilson 1999, blue).

the m/z 17 spectra used gain step 16. Thus, a gain step correction was needed. The gain step corrections were calibrated with data acquired shortly before this period (Schroeder et al. 2019a). Gain step 16 was used as the baseline by Schroeder et al. (2019a) for the gain step corrections. Consequently, the gain step correction was simple for the ratio calculated from the data considered here. On m/z 17, $^{13}CH_4$ and CH_3D are slightly over-lapping and a clear distinction is not always straightforward. This additional uncertainty has been included in the overall uncertainty.

The $^{13}C/^{12}C$ ratio has already been evaluated several times for 67P by Hässig et al. (2017) and Rubin et al. (2017) for carbon dioxide (CO_2), carbon monoxide (CO), ethylene (C_2H_4) and the ethyl radical C_2H_5 and has been shown to be independent of the parent molecule. Hence, the value of $^{13}C/^{12}C = (1.19 \pm 0.06) \times 10^{-2}$ derived from CO_2 by Hässig et al. (2017) will be used as a comparison for the values derived in this work.

From the measurements of CH_4, $^{13}CH_4$ and CH_3D, the D/H and $^{13}C/^{12}C$ ratios could be derived by taking into account the statistical correction for the four possible positions the D atom can take in the molecule. An average value of D/H = $(2.41 \pm 0.29) \times 10^{-3}$ is found in methane (Fig. 4 and Table 4). This is 4.8 times larger than the D/H ratio from HDO/H_2O but 7.5 times smaller than the D/H ratio from D_2O/HDO (Altwegg et al. 2017). The corresponding ratio of $^{13}C/^{12}C$ is $(1.14 \pm 0.13) \times 10^{-2}$, which is consistent with Hässig et al. (2017). This is additional evidence of the $^{13}C/^{12}C$ ratio being independent of the parent molecule.

3.3.2. Ethane (C$_2$H$_6$)

The evaluation of ethane (C_2H_6) was very similar to the one for methane. 20 spectra with m/z 30 and m/z 31 have been evaluated for time periods in the beginning of October 2014 and during the second equinox in March 2016. Here, the gain steps were the same on both m/z spectra and no gain correction was needed. Similar to methane, an overlap between $^{13}C^{12}CH_6$ and C_2H_5D appears on m/z 31. Again, this uncertainty has been included in the overall uncertainty of the corresponding ratios. Sample spectra for m/z 30 and m/z 31 are shown in Fig. 2. It can be seen that NO and $C^{18}O$ strongly overlap and cannot be clearly separated. For this reason, they are fitted together as one peak.

Accounting for the statistical correction for the different possible positions of the rare isotopes in the molecule, an average D/H ratio of $(2.37 \pm 0.27) \times 10^{-3}$ (Fig. 4 and Table 4) and a $^{13}C/^{12}C$ ratio of $(1.08 \pm 0.12) \times 10^{-2}$ have been obtained. This is

Table 4. D/H and $^{13}C/^{12}C$ in linear alkanes.

Alkane	D/H	$^{13}C/^{12}C$
Methane	$(2.41 \pm 0.29) \cdot 10^{-3}$	$(1.14 \pm 0.13) \cdot 10^{-2}$
Ethane	$(2.37 \pm 0.27) \cdot 10^{-3}$	$(1.08 \pm 0.12) \cdot 10^{-2}$
Propane	$(2.16 \pm 0.26) \cdot 10^{-3}$	$(1.15 \pm 0.12) \cdot 10^{-2}$
Butane	$(2.05 \pm 0.38) \cdot 10^{-3}$	$(1.04 \pm 0.15) \cdot 10^{-2}$

consistent, within the uncertainties, with Hässig et al. (2017) as well as the result for methane.

3.3.3. Propane (C_3H_8)

There are 14 Spectra with m/z 44 and m/z 45 from the second equinox in March 2016 that have been evaluated for propane (C_3H_8). Sample spectra are shown in Fig. A.2. The spectra with m/z 44 contain a very large amount of CO_2. Consequently, a small gain step was automatically selected by the DFMS while acquiring these spectra. The spectra measured around m/z 45 on the other hand showed consistently lower count rates and were thus measured on a larger gain step. For this reason, a gain correction needed to be applied before the spectra could be compared. The gain steps differed by up to four gain steps as some spectra of m/z 44 were acquired with a very low gain step (i.e. gain step 11). Low gain steps were difficult to calibrate during the calibration measurements and complicate the gain step corrections. However, Hässig et al. (2017) obtained the $^{13}C/^{12}C$ ratio in CO_2 at times when the gain steps of m/z 44 and 45 were much closer. From the $^{13}C/^{12}C$ ratio in CO_2 we thus inferred a gain correction for our measurements.

After applying the gain correction and accounting for the different possible positions of the rare isotopes in the molecule, an average D/H ratio of $(2.16 \pm 0.26) \times 10^{-3}$ was found for propane (C_3H_8, Fig. 4 and Table 4). For $^{13}C/^{12}C$ from $^{13}C^{12}C_2H_8$ and C_3H_8, the value is $(1.15 \pm 0.12) \times 10^{-2}$. Again, this value is compatible with the value from Hässig et al. (2017) and the other linear alkanes.

3.3.4. Butane (C_4H_{10})

For butane (C_4H_{10}), 11 spectra with m/z 58 and m/z 59 have been evaluated from data acquired during the second equinox in March 2016. Here, a gain correction was unnecessary, as both m/z 58 and m/z 59 were measured with the highest gain available. Sample spectra for butane are shown in Fig. A.3.

Taking into account the different possible positions of the D or ^{13}C in the molecule, butane (C_4H_{10}) showed a D/H ratio of $(2.05 \pm 0.38) \times 10^{-3}$ and a $^{13}C/^{12}C$ ratio from $^{13}C^{12}C_3H_{10}$ and C_4H_{10} of $(1.04 \pm 0.15) \times 10^{-2}$ (Fig. 4 and Table 4). As with all of the other linear alkanes considered above, the $^{13}C/^{12}C$ ratio is consistent with Hässig et al. (2017) and the other linear alkanes.

4. Discussion

The ROSINA/DFMS measurements show that the D/H ratio in water does not change during 67P's passage around the Sun between May 2015 and March 2016. It is clear, that the instrument's observations represent an average of the illuminated surface, even though they have been measured at different positions. Hence, we cannot examine any point-to-point variability on the surface itself. However, given the large variability of the phase angles and sub-S/C latitudes during the evaluated measurement phases and their association with different spacecraft distances to the comet, we can conclude that the D/H ratio in water in 67P's coma is independent of heliocentric distance, level of cometary activity, and Rosetta's phase angle as well as sub-S/C latitude (Fig. 3). The relative overall mean value, considering only statistical and fit uncertainties, has a 1σ variation of 2.0% with all investigated periods being consistent. The derived D/H ratio for water is compatible with values previously published in Altwegg et al. (2015, 2017). However, the new values presented in this work are based on a larger number of measurements and hence have smaller error margins. The most accurate absolute value for D/H in HDO/H_2O we obtained from our data is $(5.01 \pm 0.40) \times 10^{-4}$, where the uncertainty includes all statistical and systematic uncertainties.

Paganini et al. (2017) and Biver et al. (2016) reported different values for the D/H ratio in water for comet Lovejoy pre- and post-perihelion. Paganini et al. (2017) favoured the explanation of a systematic difference between the two observations by Biver et al. (2016) as a reason for the changing D/H ratio observed for comet Lovejoy. If the results for comet 67P are valid for other comets, our study indicates a constant D/H ratio, within the uncertainties, and therefore supports the hypothesis of a systematic difference rather than a change in the D/H ratio of comet Lovejoy.

Lis et al. (2019) proposed that the D/H ratio in cometary water correlates with the nucleus' active area fraction. Fulle (2021) modelled this scenario and suggested that the fraction of water-rich and water-poor pebbles influences the D/H ratio in the comet's coma. The data evaluated for this paper show that the D/H ratio is independent of 67P's activity (in the form of H_2O outgassing) and Rosetta's relative position in terms of phase angle and sub-spacecraft latitude; hence, the data do not show any signs of such a scenario for 67P.

Measurements taken of the first four linear alkanes in 67P's coma show that their D/H ratios are all consistent within the uncertainties. The derived values are larger than the aforementioned ratio obtained from HDO/H_2O by a factor of 4.1 to 4.8, but smaller than the D/H ratio obtained from D_2O/HDO (Altwegg et al. 2017). In addition, the D/H ratio in the alkanes is slightly larger than the ratio obtained from HDS (Altwegg et al. 2017) but it is still on the same order of magnitude. The first-time detection of mono- and di-deuterated methanol in a cometary coma was published by Drozdovskaya et al. (2021). The authors evaluated Rosetta/ROSINA data for 67P. With the ROSINA instruments, it is not possible to distinguish between the different chemical compositions of D-methanol (CH_3OD and CH_2DOH) and D_2-methanol (CH_2DOD and CHD_2OH), respectively. Moreover, different approaches for the calculation of the D/H ratio in methanol are possible and it cannot be judged which of the pathways is more reliable. Consequently, although it was not possible to deduce a single D/H ratio in CH_3OH, a range of 0.71-6.6 per cent was given by the authors. This accounts for the different isomers of methanol and includes statistical error propagation in the ROSINA measurements. The authors propose that methanol and its deuterated isotopologues in comet 67P must have formed in the prestellar core that preceded our Solar System and at a time when it was at a temperature of 10–20 K. Moreover, it is assumed that methanol is a pivotal precursor to complex organic molecules, and hence, could be a source of deuterium for such species (Oba et al. 2016). The presented D/H value in methanol is much larger than the ratios obtained for the first four linear alkanes. However, Drozdovskaya et al. (2021) demonstrate that the upper boundary of 6.6% of their determined D/H range
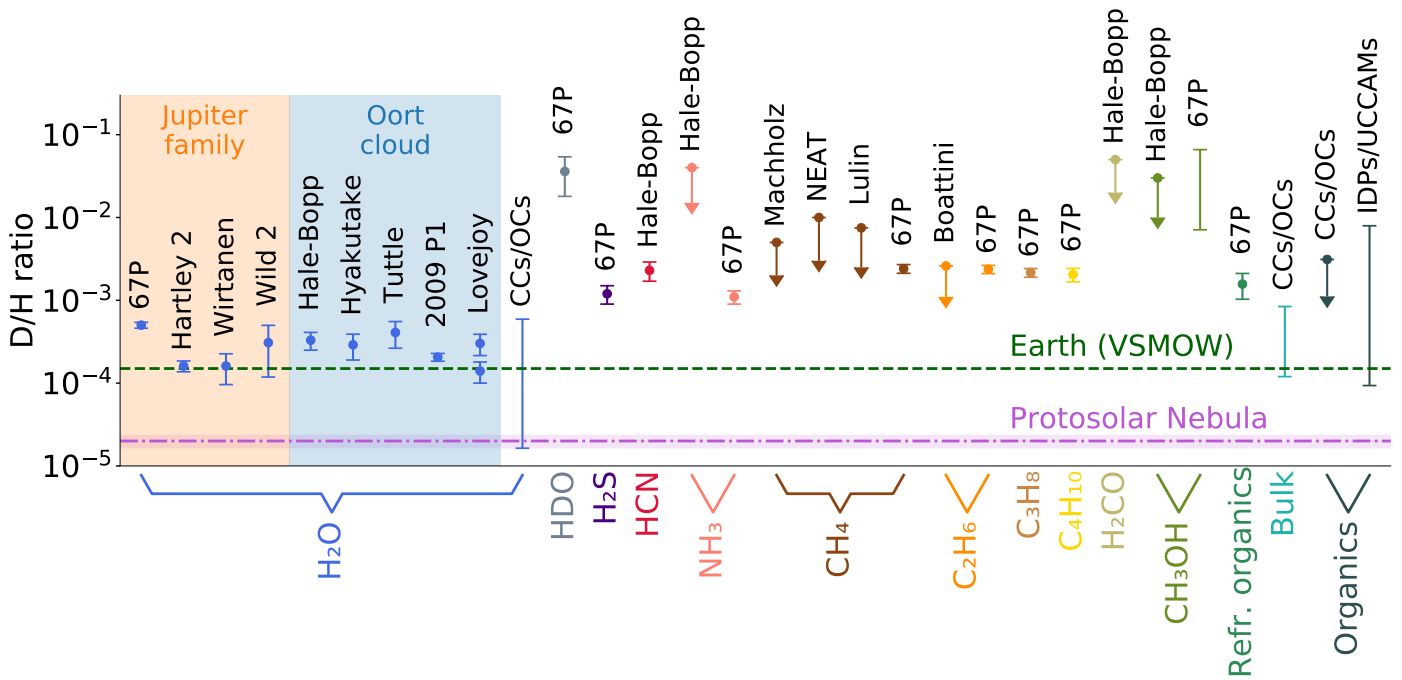
Fig. 5. D/H ratios of water and organic molecules measured in different comets compared to values from the Protosolar Nebula (purple line, Geiss & Gloeckler 2003), the Earth (green line, Wilson 1999), carbonaceous chondrites (CC), ordinary chondrites (OC), interplanetary dust particles (IDP) and ultracarbonaceous Antarctic micrometeorites (UCCAM). D/H in HDO is equal to $2 \cdot D_2O/HDO$. Full references are given in Table B.1.

would only apply in the extreme case where all D-methanol was in the form of CH_3OD. In the much more likely case that D-methanol exists in the form of different isomers (Ratajczak et al. 2011), the D/H in methanol would be lower and thus comparable to the D_2O/HDO ratio of $(1.8 \pm 0.9) \cdot 10^{-2}$ from Altwegg et al. (2017).

Furuya et al. (2016) have described the development of ice structures during the formation of protostellar cores with two layers from molecular clouds. The first layer is the main formation stage of H_2O ice. The second, outer layer is CO/CH_3OH-rich and includes material that underwent enhanced deuteration processes due to low temperatures (T < 20 K). Their model shows higher levels of deuterium fractionation of formaldehyde and methanol from the outer layer than in water in the inner layer and gives similar D/H ratios for methanol and D_2O. They suggest that this difference reflects the epochs of the molecules' formation as water ice is formed at an earlier stage of protostellar cloud condensation at elevated temperatures than the ices of formaldehyde and methanol. These conclusions might explain why at 67P the D/H ratios for D_2O/HDO and methanol are similar but much larger compared to D/H in H_2O. The way in which such a scenario would affect the deuteration in hydrocarbons, however, requires further investigation.

Measurements of organics in other comets, for instance, the D/H ratio in HCN in comet C/1995 O1 (Hale-Bopp) (Crovisier et al. 2004) match the values for the first four linear alkanes within the uncertainties.

Paquette et al. (2021) presented the first in situ measurements of the D/H ratios in organic refractory components of cometary dust particles. These cometary dust particles have been captured on metal targets within the coma of comet 67P. The particles were then imaged by a microscope camera and a fraction of them were analysed with the Cometary Secondary Ion Mass Analyzer (COSIMA), a time-of-flight secondary ion mass spectrometer (Kissel et al. 2007). The incident velocities of the

particles COSIMA collected were low and they did not suffer a high degree of thermal alteration. Greater thermal alterations occur in flyby missions, where incident velocities experienced by particles are larger by several orders of magnitude (Paquette et al. 2021). The D/H ratio of $(1.57 \pm 0.54) \times 10^{-3}$ in the organic refractory components of 67P's cometary dust is comparable to our D/H ratios in linear alkanes. It is thus also about an order of magnitude higher than the VSMOW for the D/H ratio on Earth. Paquette et al. (2021) have stated, that this relatively high value puts forward the theory that refractory carbonaceous matter in comet 67P is less processed than the most primitive insoluble organic matter (IOM) in meteorites.

Bonev et al. (2009) reported an upper limit of 5×10^{-3} for the D/H ratio in methane in comet C/2004 Q2 (Machholz), while Kawakita et al. (2005) determined an upper limit for the D/H ratio of 1×10^{-2} for comet C/2001 Q4 (NEAT), and Gibb et al. (2012) found an upper limit of 7.5×10^{-3} for comet C/2007 N3 (Lulin). The D/H ratio we determined in methane for 67P is about a factor of two lower than the smallest previously obtained upper limit for this molecule.

An upper limit for the D/H ratio in ethane of 2.6×10^{-3} from modelled emission spectra of comet C/2007 W1 (Boattini) has been determined by Doney et al. (2020). Hence, for ethane, our D/H ratio for 67P is comparable to this upper limit.

This work is the first to present an isotopic ratio for methane, ethane, propane, and butane for comets. No other values are available for comparison.

A comparison of the D/H ratios investigated here with values obtained from different comets and on different organic molecules is shown in Fig. 5. D/H ratios from the Protosolar Nebula, Earth, carbonaceous chondrites (CC), ordinary chondrites (OC), interplanetary dust particles (IDP) and ultracarbonaceous Antarctic micrometeorites (UCCAM) are added for comparison. The D/H ratio from HDO/H_2O is larger for most of the observed comets compared to the terrestrial value, though they
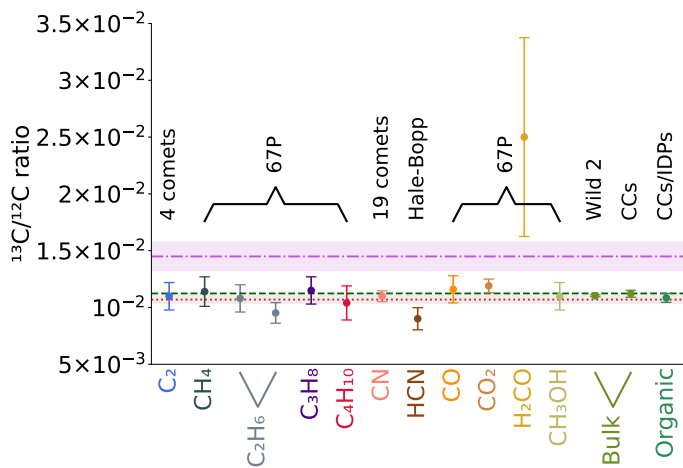
Fig. 6. $^{13}C/^{12}C$ ratios of different organic molecules measured in different comets, carbonaceous chondrites (CC) and interplanetary dust particles (IDP) compared to the terrestrial value (green line, Lyons et al. 2018), the Sun (brown line, Lyons et al. 2018) and the ISM (purple line, Wilson 1999). For C_2 and CN, data from 4 and 19 comets, respectively, have been considered. Full references are given in Table B.2.

Fig. 7. D/H ratios compared to $^{13}C/^{12}C$ ratios of different organic molecules measured in comets 67P and Hale-Bopp and in bulk and organic carbonaceous chondrites (CC). Full references are given in Table B.1 for the D/H ratios and in Table B.2 for the $^{13}C/^{12}C$ ratios.

show large variations. Variations are also observed within the comet families, the JFCs and the Oort cloud comets (OCC). It also seems that organic compounds in the comets investigated exhibit even larger D/H ratios than water. A comparison of the D/H ratios derived from cometary organics, chondrites, and IDPs to values from the Protosolar Nebula and the VSMOW reveals a pronounced deuterium enrichment in Solar System objects in general. Hoppe et al. (2018) suggested that 67P might be particularly primordial and might have conserved large amounts of presolar matter due to the fact that its D/H ratio corresponds to the highest values proposed for comets to date. Water in chondrites has D/H ratios in between those of the Protosolar Nebula and the highest cometary values. On the other hand, chondritic IOM shows strong D-enrichment as compared to VSMOW. According to Alexander et al. (2010), this deuterium enrichment is not a signature of the primordial H in the presolar cloud, but is caused by different processes. Moreover, Duprat et al. (2010) analysed ultracarbonaceous micrometeorites recovered from central Antarctic snow and found extreme deuterium enrichment in large areas of the organic matter contained therein. In addition, crystalline minerals embedded in the micrometeoritic organic matter have been identified. According to the authors, this suggests that this organic matter reservoir may have formed within the Solar System itself and was not inherited from presolar times. As a summary of their findings, the high D/H ratios, the high organic matter content, and the associated minerals are said to favour an origin from the cold regions of the protoplanetary disc (Duprat et al. 2010).

According to Cleeves et al. (2016), the D/H ratio in both water and organics can become chemically enhanced in cold environments exposed to ionising radiation. The authors proposed the cold interstellar medium, activated by galactic cosmic rays, and the outermost regions of the protoplanetary disc in the presence of stellar or non-stellar ionisation, as two possible environments where this deuterium enrichment could occur. In an earlier study, Cleeves et al. (2014) state that a considerable fraction of the Solar System's water predates the Sun and that a certain amount of such interstellar ice survived the formation of the Solar System and has been incorporated into planetesimals. The authors also identified two factors which might lead
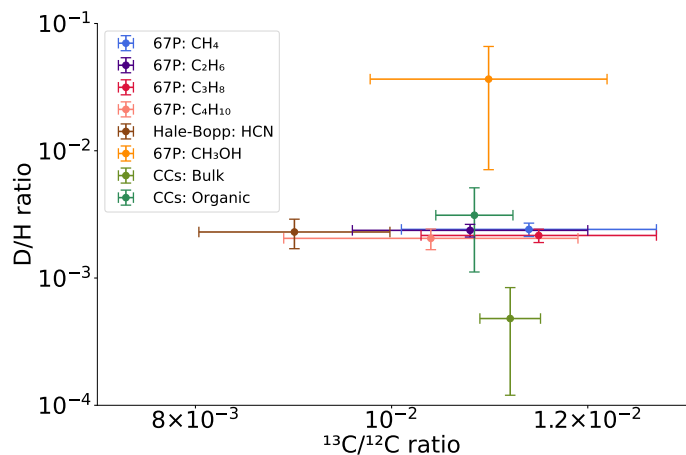
to the even higher degree of deuterium enrichment in protoplanetary disc organics as compared to water: (1) the higher volatility and abundance of CO, which is the main carbon reservoir, as compared to O (atomic oxygen), which is the main precursor for water formation, and, (2) a more favourable chemistry for deuterium-fractionation in organics than in water due to a higher exothermicity in the chemical formation reaction (Cleeves et al. 2016).

Embedded protostars in low-mass star-forming regions exhibit D/H ratios in their water on a level that is similar to the values found for comets (Persson et al. 2014). On the other hand, isolated protostars have D/H ratios of more than double the values observed in embedded protostars (Jensen et al. 2019), and their D/H ratios are thus more similar to those of cometary organics. The high D/H ratios in cometary organic compounds generally suggest that these species may be inherited from the presolar molecular cloud from which the Solar System formed.

The alkanes investigated show $^{13}C/^{12}C$ ratios compatible with published values for CO (Rubin et al. 2017) and CO_2 (Hässig et al. 2017) in 67P and the $^{13}C/^{12}C$ ratio in the Solar System (Wilson 1999). Altwegg et al. (2020) found a $^{13}C/^{12}C$ ratio in ethane of $(0.95 \pm 0.1) \times 10^{-2}$ which matches the results presented in this work within the uncertainties. These authors also revealed that the $^{13}C/^{12}C$ ratio varies for different molecules in 67P's coma, but that, except for H_2CO with its large uncertainty, the $^{13}C/^{12}C$ ratios are in the same range as our values. This picture is supported by data from other comets and even bulk and organic CCs, where the $^{13}C/^{12}C$ ratios for different molecules are similar (Bockelée-Morvan et al. 2015; Hoppe et al. 2018). A comparison of $^{13}C/^{12}C$ ratios for different organic molecules measured in different comets and other Solar System objects is shown in Fig. 6. All these values lie below the local ISM value (Wilson 1999) but are mostly compatible with the terrestrial and the solar value (Lyons et al. 2018). This indicates that isotopic fractionation may have occurred over time and was, at least for most organic molecules, independent of the molecular structure.

In conjunction with the small variations in the $^{13}C/^{12}C$ ratios and the large variations in the D/H ratios, Fig. 7 illustrates that there is no correlation between the $^{13}C/^{12}C$ ratio and the D/H ratio for comets and CCs.

5. Summary and conclusions

In this work, we investigate the isotopic ratios of water and the four simplest alkanes found in the inner coma of comet 67P. The most relevant findings can be summarised as follows:

- The D/H ratio in water in 67P's coma, measured with ROSINA/DFMS, is independent of the heliocentric distance, the level of cometary activity, the spacecraft's phase angle and the sub-spacecraft latitude.

- A 1σ variation of 2.0% is included in the relative overall mean value. All the values derived from the investigated periods are consistent with this value.

- From our data, we obtained an absolute D/H ratio from HDO/H_2O of $(5.01\pm0.40)\times10^{-4}$. Many comets exhibit larger D/H ratios in water as compared to the terrestrial value. However, both cometary families, JFCs and OCCs, also include comets with values comparable to the VSMOW value. Hence, the implications for cometary contributions to terrestrial water remain unclear if only cometary water is examined.

- The $^{16}O/^{17}O$ ratio in water in 67P's coma was determined to be constant throughout the mission, with a relative 1σ variation of 2.3%. An absolute $^{16}O/^{17}O$ ratio of 2347 ± 191 has been found.

- The four simplest linear alkanes show larger D/H ratios than 67P's water by a factor of 4.1 to 4.8. Their D/H ratio values are consistent with data from other organic molecules and from different comets.

- A comparison between different sources of cometary matter showed that organic molecules generally exhibit higher D/H ratios than water for all comets reviewed in this work.

- No correlation was found between the $^{13}C/^{12}C$ ratio and the D/H ratio for different cometary molecules.

The observed invariability of the D/H ratio in 67P's coma opposes theories of a non-steady-state regime of water ice sublimation occurring in sporadic time intervals along the comet's orbit. However, this invariability needs to be confirmed for other comets with further measurements and with other measurement approaches. Additionally, 67P's close apparition in November 2021 has been an excellent opportunity to re-measure the D/H ratio using spectroscopic approaches and upcoming results are highly anticipated. On the other hand, to further constrain the history and origin of organic matter in the Solar System, more data from comets and other Solar System objects ought to be analysed and more studies are required to investigate these species' formation pathways.

References

Alexander, C. M. O., Bowden, R., Fogel, M. L., et al. 2012, Science, 337, 721
Alexander, C. M. O. D., Fogel, M., Yabuta, H., & Cody, G. D. 2007, Geochim. Cosmochim. Acta, 71, 4380
Alexander, C. M. O. D., Newsome, S. D., Fogel, M. L., et al. 2010, Geochim. Cosmochim. Acta, 74, 4417
Altwegg, K., Balsiger, H., Bar-Nun, A., et al. 2015, Science, 347, 1261952
Altwegg, K., Balsiger, H., Berthelier, J. J., et al. 2017, Philosophical Transactions of the Royal Society of London Series A, 375, 20160253
Altwegg, K., Balsiger, H., Combi, M., et al. 2020, MNRAS, 498, 5855
Altwegg, K., Balsiger, H., & Fuselier, S. A. 2019, ARA&A, 57, 113
Balsiger, H., Altwegg, K., Bochsler, P., et al. 2007, Space Sci. Rev., 128, 745
Biver, N., Bockelée-Morvan, D., Hofstadter, M., et al. 2019, A&A, 630, A19
Biver, N., Moreno, R., Bockelée-Morvan, D., et al. 2016, A&A, 589, A78
Bockelée-Morvan, D., Calmonte, U., Charnley, S., et al. 2015, Space Sci. Rev., 197, 47
Bockelée-Morvan, D., Gautier, D., Lis, D. C., et al. 1998, Icarus, 133, 147
Bonev, B. P., Mumma, M. J., Gibb, E. L., et al. 2009, ApJ, 699, 1563
Busemann, H., Young, A. F., O'D. Alexander, C. M., et al. 2006, Science, 312, 727
Calmonte, U., Altwegg, K., Balsiger, H., et al. 2016, MNRAS, 462, S253
Calmonte, U., Altwegg, K., Balsiger, H., et al. 2017, MNRAS, 469, S787
Clark, R. N., Curchin, J. M., Hoefen, T. M., & Swayze, G. A. 2009, Journal of Geophysical Research (Planets), 114, E03001
Cleeves, L. I., Bergin, E. A., Alexander, C. M. O. D., et al. 2014, Science, 345, 1590
Cleeves, L. I., Bergin, E. A., O'D. Alexander, C. M., et al. 2016, ApJ, 819, 13
Combi, M., Shou, Y., Fougere, N., et al. 2020, Icarus, 335, 113421
Crovisier, J., Bockelée-Morvan, D., Colom, P., et al. 2004, A&A, 418, 1141
De Keyser, J., Altwegg, K., Gibbons, A., et al. 2019, International Journal of Mass Spectrometry, 446, 116232
Dhooghe, F., De Keyser, J., Altwegg, K., et al. 2017, MNRAS, 472, 1336
Doney, K., Kofman, V., Villanueva, G., & Sung, K. 2020, in American Astronomical Society Meeting Abstracts, Vol. 235, American Astronomical Society Meeting Abstracts #235, 226.06
Drozdovskaya, M. N., Schroeder I, I. R. H. G., Rubin, M., et al. 2021, MNRAS, 500, 4901
Drozdovskaya, M. N., van Dishoeck, E. F., Rubin, M., Jørgensen, J. K., & Altwegg, K. 2019, MNRAS, 490, 50
Duprat, J., Dobrică, E., Engrand, C., et al. 2010, Science, 328, 742
Feller, C., Fornasier, S., Ferrari, S., et al. 2019, A&A, 630, A9
Floss, C. & Stadermann, F. J. 2004, in Lunar and Planetary Science Conference, ed. S. Mackwell & E. Stansbery, Lunar and Planetary Science Conference, 1281
Fulle, M. 2021, MNRAS, 505, 3107
Furuya, K., Aikawa, Y., Nomura, H., Hersant, F., & Wakelam, V. 2013, ApJ, 779, 11
Furuya, K., van Dishoeck, E. F., & Aikawa, Y. 2016, A&A, 586, A127
Geiss, J. & Gloeckler, G. 2003, Space Sci. Rev., 106, 3
Geiss, J. & Reeves, H. 1981, A&A, 93, 189
Gibb, E. L., Bonev, B. P., Villanueva, G., et al. 2012, ApJ, 750, 102
Goesmann, F., Rosenbauer, H., Bredehöft, J. H., et al. 2015, Science, 349, 2.689
Hartogh, P., Lis, D. C., Bockelée-Morvan, D., et al. 2011, Nature, 478, 218
Hässig, M., Altwegg, K., Balsiger, H., et al. 2017, A&A, 605, A50
Hässig, M., Altwegg, K., Balsiger, H., et al. 2013, Planet. Space Sci., 84, 148
Hässig, M., Altwegg, K., Berthelier, J. J., et al. 2015, Planet. Space Sci., 105, 175
Herny, C., Mousis, O., Marschall, R., et al. 2021, Planet. Space Sci., 200, 105194
Hoppe, P., Rubin, M., & Altwegg, K. 2018, Space Sci. Rev., 214, 106
Jensen, S. S., Jørgensen, J. K., Kristensen, L. E., et al. 2019, A&A, 631, A25
Jewitt, D., Matthews, H. E., Owen, T., & Meier, R. 1997, Science, 278, 90
Kavelaars, J. J., Mousis, O., Petit, J.-M., & Weaver, H. A. 2011, ApJ, 734, L30
Kawakita, H., Watanabe, J.-i., Furusho, R., Fuse, T., & Boice, D. C. 2005, ApJ, 623, L49
Kawakita, H., Watanabe, J.-i., Kinoshita, D., Ishiguro, M., & Nakamura, R. 2003, ApJ, 590, 573
Keller, H. U., Mottola, S., Davidsson, B., et al. 2015, A&A, 583, A34
Kerridge, J. F. 1985, Geochim. Cosmochim. Acta, 49, 1707
Kissel, J., Altwegg, K., Clark, B. C., et al. 2007, Space Sci. Rev., 128, 823
Läuter, M., Kramer, T., Rubin, M., & Altwegg, K. 2020, MNRAS, 498, 3995
Le Roy, L., Altwegg, K., Balsiger, H., et al. 2015, A&A, 583, A1
Lis, D. C., Bockelée-Morvan, D., Güsten, R., et al. 2019, A&A, 625, L5
Longobardo, A., Della Corte, V., Rotundi, A., et al. 2020, MNRAS, 496, 125
Lunine, J. I. & Atreya, S. K. 2008, Nature Geoscience, 1, 159
Lyons, J. R., Gharib-Nezhad, E., & Ayres, T. R. 2018, Nature Communications, 9, 908
Manfroid, J., Jehin, E., Hutsemékers, D., et al. 2009, A&A, 503, 613
McKeegan, K. D., Aléon, J., Bradley, J., et al. 2006, Science, 314, 1724
Meier, R., Owen, T. C., Matthews, H. E., et al. 1998, Science, 279, 842

Meija, J., Coplen, T. B., Berglund, M., et al. 2016, Pure and Applied Chemistry, 88, 293

Messenger, S. 2000, Nature, 404, 968

Mumma, M. J. & Charnley, S. B. 2011, ARA&A, 49, 471

Mumma, M. J., Disanti, M. A., dello Russo, N., et al. 1996, IAU Circ., 6366, 1

Nevejans, D., Neefs, E., Kavadias, S., Merken, P., & Van Hoof, C. 2002, International Journal of Mass Spectrometry, 215, 77

Oba, Y., Takano, Y., Watanabe, N., & Kouchi, A. 2016, ApJ, 827, L18

Paganini, L., Mumma, M. J., Gibb, E. L., & Villanueva, G. L. 2017, ApJ, 836, L25

Paquette, J. A., Fray, N., Bardyn, A., et al. 2021, MNRAS, 504, 4940

Pearson, V. K., Sephton, M. A., Gilmour, I., & Franchi, I. A. 2001, in Lunar and Planetary Science Conference, Lunar and Planetary Science Conference, 1861

Persson, M. V., Jørgensen, J. K., van Dishoeck, E. F., & Harsono, D. 2014, A&A, 563, A74

Pestoni, B., Altwegg, K., Balsiger, H., et al. 2021, A&A, 645, A38

Ratajczak, A., Taquet, V., Kahane, C., et al. 2011, A&A, 528, L13

Rubin, M., Altwegg, K., Balsiger, H., et al. 2017, A&A, 601, A123

Rubin, M., Altwegg, K., Balsiger, H., et al. 2019, MNRAS, 489, 594

Schroeder, I. R. H. G., Altwegg, K., Balsiger, H., et al. 2019a, MNRAS, 489, 4734

Schroeder, I. R. H. G., Altwegg, K., Balsiger, H., et al. 2019b, A&A, 630, A29

Schuhmann, M., Altwegg, K., Balsiger, H., et al. 2019, A&A, 630, A31

Stadermann, F. J., Hoppe, P., Floss, C., et al. 2008, Meteoritics & Planetary Science, 43, 299

Sunshine, J. M. & Feaga, L. M. 2021, The Planetary Science Journal, 2, 92

Wilson, T. L. 1999, Reports on Progress in Physics, 62, 143

Wright, I. P., Sheridan, S., Barber, S. J., et al. 2015, Science, 349, 2.673

Wyckoff, S. 1991, Earth Science Reviews, 30, 125

Wyckoff, S., Kleine, M., Peterson, B. A., Wehinger, P. A., & Ziurys, L. M. 2000, ApJ, 535, 991

Yang, J. & Epstein, S. 1984, Nature, 311, 544

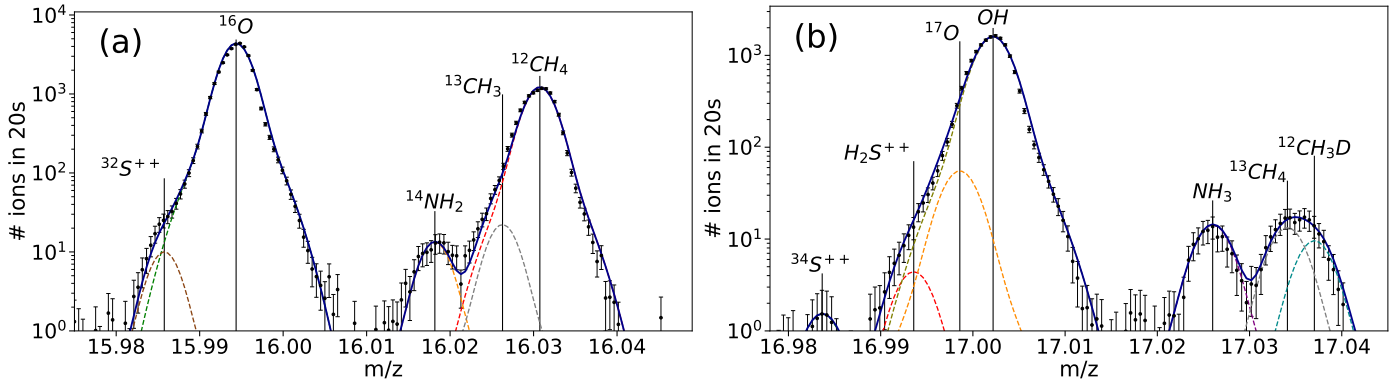# Appendix A: Mass spectra showing signatures of methane, propane and butane and their isotopologues

Fig. A.1. Sample mass spectra for *m/z* 16 and 17 showing the signatures of the isotopologues of methane. *Panel a*: *m/z* 16 from 2016-03-09 11:13 (UTC). *Panel b*: *m/z* 17 from 2016-03-09 11:14 (UTC). Measured data are represented by black dots including their statistical uncertainties. The individual mass fits and the total sum of the fits are shown with coloured lines.
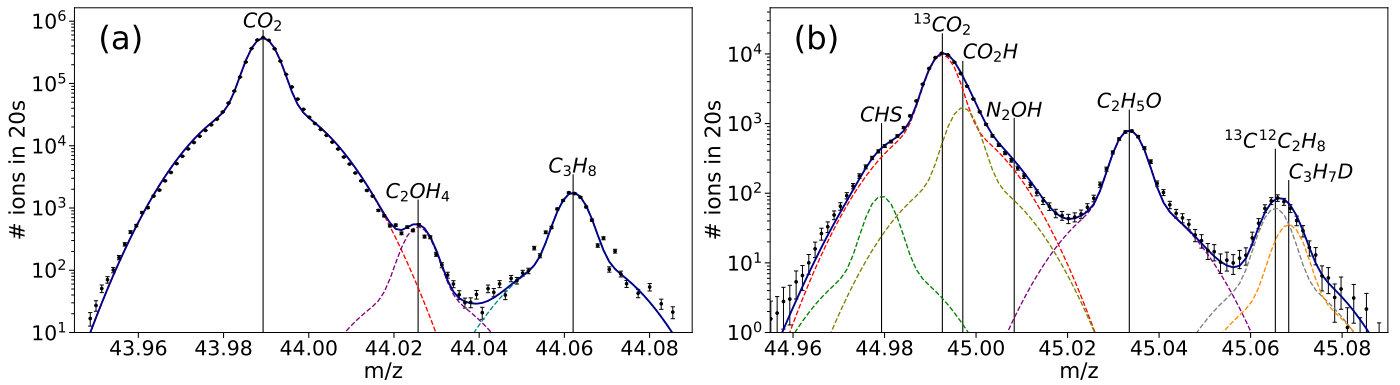
Fig. A.2. Sample mass spectra for *m/z* 44 and 45 showing the signatures of the isotopologues of propane. *Panel a*: *m/z* 44 from 2016-03-20 15:24 (UTC). *Panel b*: *m/z* 45 from 2016-03-20 15:24 (UTC). Measured data are represented by black dots including their statistical uncertainties. The individual mass fits and the total sum of the fits are shown with coloured lines.

Fig. A.3. Sample mass spectra for *m/z* 58 and 59 showing the signatures of the isotopologues of butane. *Panel a*: *m/z* 58 from 2016-03-19 22:45 (UTC). *Panel b*: *m/z* 59 from 2016-03-19 22:45 (UTC). Measured data are represented by black dots including their statistical uncertainties. The individual mass fits and the total sum of the fits are shown with coloured lines.
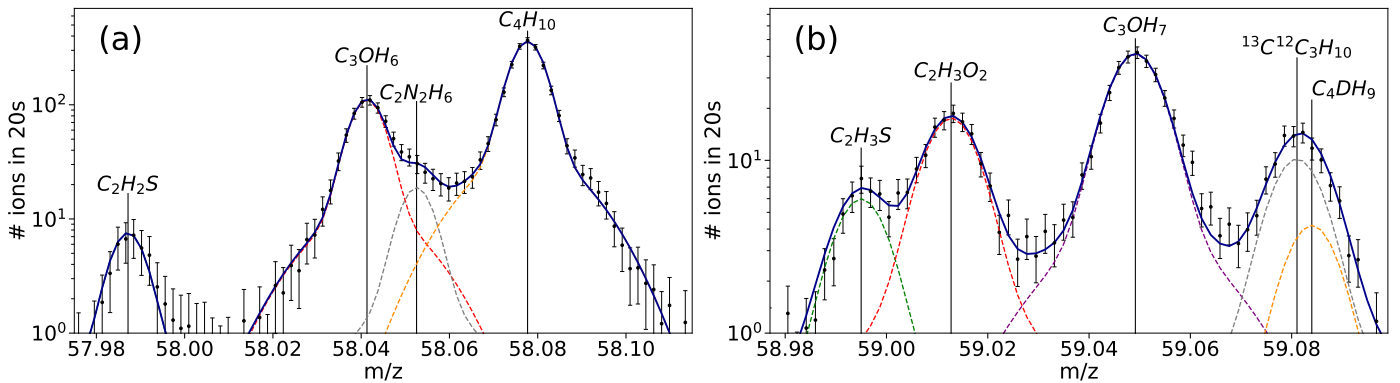
Appendix B: Reference tables for literature values used in figures

Table B.1. Literature values for D/H in comets, CCs and IDPs.

Molecule	Source	D/H	Reference
H_2O	67P	$(5.01 \pm 0.41) \cdot 10^{-4}$	This work
H_2O	103P/Hartley 2	$(1.61 \pm 0.24) \cdot 10^{-4}$	Hartogh et al. (2011)
H_2O	46P/Wirtanen	$(1.61 \pm 0.65) \cdot 10^{-4}$	Lis et al. (2019)
H_2O	81P/Wild 2	$(1.18 - 4.98) \cdot 10^{-4}$	McKeegan et al. (2006)
H_2O	C/1995 O1 (Hale-Bopp)	$(3.3 \pm 0.8) \cdot 10^{-4}$	Meier et al. (1998)
H_2O	C/1996 B2 (Hyakutake)	$(2.9 \pm 1) \cdot 10^{-4}$	Bockelée-Morvan et al. (1998)
H_2O	8P/Tuttle	$(4.09 \pm 1.45) \cdot 10^{-4}$	Bockelée-Morvan et al. (2015)
H_2O	C/2009 P1 (Garradd)	$(2.06 \pm 0.22) \cdot 10^{-4}$	Bockelée-Morvan et al. (2015)
H_2O	C/2014 Q2 (Lovejoy)	$(1.4 \pm 0.4) \cdot 10^{-4}$	Biver et al. (2016)
H_2O	C/2014 Q2 (Lovejoy)	$(3.02 \pm 0.87) \cdot 10^{-4}$	Paganini et al. (2017)
H_2O	CCs/OCs	$(0.16 - 5.9) \cdot 10^{-4}$	Alexander et al. (2010, 2012)
$HDO^{[a]}$	67P	$(3.6 \pm 1.8) \cdot 10^{-2}$	Altwegg et al. (2017)
H_2S	67P	$(1.2 \pm 0.3) \cdot 10^{-3}$	Altwegg et al. (2017)
HCN	C/1995 O1 (Hale-Bopp)	$(2.3 \pm 0.6) \cdot 10^{-3}$	Crovisier et al. (2004)
NH_3	C/1995 O1 (Hale-Bopp)	$< 4 \cdot 10^{-2}$	Crovisier et al. (2004)
NH_3	67P	$(1.1 \pm 0.2) \cdot 10^{-3}$	Altwegg et al. (2019)
CH_4	C/2004 Q2 (Machholz)	$< 5 \cdot 10^{-3}$	Bonev et al. (2009)
CH_4	C/2001 Q4 (NEAT)	$< 1 \cdot 10^{-2}$	Kawakita et al. (2005)
CH_4	C/2007 N3 (Lulin)	$< 7.5 \cdot 10^{-3}$	Gibb et al. (2012)
CH_4	67P	$(2.41 \pm 0.29) \cdot 10^{-3}$	This work
C_2H_6	C/2007 W1 (Boattini)	$< 2.6 \cdot 10^{-3}$	Doney et al. (2020)
C_2H_6	67P	$(2.37 \pm 0.27) \cdot 10^{-3}$	This work
C_3H_8	67P	$(2.16 \pm 0.26) \cdot 10^{-3}$	This work
C_4H_{10}	67P	$(2.05 \pm 0.38) \cdot 10^{-3}$	This work
H_2CO	C/1995 O1 (Hale-Bopp)	$< 5 \cdot 10^{-2}$	Crovisier et al. (2004)
CH_3OH	C/1995 O1 (Hale-Bopp)	$< 3 \cdot 10^{-2}$	Crovisier et al. (2004)
CH_3OH	67P	$(0.71 - 6.63) \cdot 10^{-2}$	Drozdovskaya et al. (2021)
Refr. Organics	67P	$(1.57 \pm 0.54) \cdot 10^{-3}$	Paquette et al. (2021)
Bulk	CCs/OCs	$(1.2 - 8.4) \cdot 10^{-3}$	Alexander et al. (2010, 2012); Kerridge (1985); Pearson et al. (2001); Yang & Epstein (1984)
Organics	CCs/OCs	$< 3.1 \cdot 10^{-3}$	Alexander et al. (2007, 2010); Busemann et al. (2006)
Organics	IDPs/UCCAMs	$9 \cdot 10^{-5} - 8 \cdot 10^{-3}$	Duprat et al. (2010); Messenger (2000)

References. (a) D/H in HDO is equal to $2 \cdot D_2O/HDO$

Table B.2. Literature values for $^{13}C/^{12}C$ in comets, CCs and IDPs.

Molecule	Source	$^{13}C/^{12}C$	Reference
C_2	4 comets	$(1.10 \pm 0.12) \cdot 10^{-2}$	Wyckoff et al. (2000)
CH_4	67P	$(1.14 \pm 0.13) \cdot 10^{-2}$	This work
C_2H_6	67P	$(1.08 \pm 0.12) \cdot 10^{-2}$	This work
C_2H_6	67P	$(9.5 \pm 0.9) \cdot 10^{-3}$	Altwegg et al. (2020)
C_3H_8	67P	$(1.15 \pm 0.12) \cdot 10^{-2}$	This work
C_4H_{10}	67P	$(1.04 \pm 0.15) \cdot 10^{-2}$	This work
CN	19 comets	$(1.10 \pm 0.05) \cdot 10^{-2}$	Manfroid et al. (2009)
HCN	C/1995 O1 (Hale-Bopp)	$(9.0 \pm 1.0) \cdot 10^{-3}$	Jewitt et al. (1997)
CO	67P	$(1.16 \pm 0.12) \cdot 10^{-2}$	Rubin et al. (2017)
CO_2	67P	$(1.19 \pm 0.06) \cdot 10^{-2}$	Hässig et al. (2017)
H_2CO	67P	$(2.5 \pm 0.9) \cdot 10^{-2}$	Altwegg et al. (2020)
CH_3OH	67P	$(1.10 \pm 0.12) \cdot 10^{-2}$	Altwegg et al. (2020)
Bulk	81P/Wild 2	$(1.1 \pm 0.01) \cdot 10^{-2}$	Stadermann et al. (2008)
Bulk	CCs	$(1.09 - 1.15) \cdot 10^{-2}$	Alexander et al. (2010, 2012); Pearson et al. (2001)
Organics	CCs/IDPs	$(1.05 - 1.12) \cdot 10^{-2}$	Alexander et al. (2007); Floss & Stadermann (2004)